Synthesis of nondiffracting beams in free space

Joseph Rosen*

Optical Signal Processing Branch, Rome Laboratory, Hanscom Air Force Base, Massachusetts 01731

Received September 29, 1993

A novel method of designing the longitudinal intensity profile of a diffracted beam in free space is proposed. By use of this method illumination of an arbitrarily synthesized aperture can yield a desired intensity distribution, including a constant (nondiffracting) curve, along a chosen limited range.

In 1987 the so-called nondiffering beam was discovered by Durnin.[1] This beam, with initial transversal distribution of a truncated zero-order Bessel function, propagates in free space, while the central spot intensity along the longitudinal axis remains approximately unchanged for a much longer distance than that of a similar Gaussian beam. Since that time some other beam functions with interesting propagation properties were studied,[2–5] and different methods of implementation were proposed.[6–11]

In this Letter we propose a general method of designing the intensity profile along the propagation axis of a beam diffracted from an arbitrary aperture. As a special case, we demonstrate the technique on a narrow and intense spot beam with a weak and wide background level. In this example the chosen intensity distribution along the longitudinal axis is a constant level along some selected interval. As we demonstrate, our technique improves the properties of the original Durnin nondiffracting beam. In what follows, the method is described, starting from the scalar diffraction theory.

Based on the Rayleigh–Sommerfeld formula the complex amplitude distribution along the longitudinal axis z of a beam diffracted from an aperture $f(r,\theta)$ is[12]

$$u(z) = \frac{1}{j\lambda}\int_0^{2\pi}\int_0^{\infty} f(r,\theta)h(r,z)r\,\mathrm{d}r\,\mathrm{d}\theta\,, \qquad (1)$$

where $h(r,z) = [\exp(jkR)/R]\cos\phi$, $R = (z^2 + r^2)^{1/2}$, $\cos\phi = z/R$, (r,θ,z) are the cylindrical coordinates of the space, λ is the wavelength, and $k = 2\pi/\lambda$ is the wave number.

Our aim is to find some initial aperture $f(r,\theta)$ that yields a desired intensity function $I_0(z) = |u(z)|^2$ along a predefined interval Δz on the z axis. We confine the search to aperture functions that possess specified properties. Therefore the problem may be defined as follows: Find the aperture distribution $f(r,\theta)$ of specified properties such that substitution of it into Eq. (1) yields, as closely as possible, the desired intensity distribution $I_0(z)$ along an interval Δz. Now we have a constrained optimization problem, which will be solved by an extended version of the projections-onto-constraint-sets (EPOCS) algorithm.[13,14]

In order to formulate the given problem in a proper form for the EPOCS we rewrite Eq. (1) as follows:

$$u(\zeta) = \frac{\sqrt{\zeta}}{2j\lambda}\int_0^{2\pi}\int_0^{\infty} f'(\rho,\theta)\frac{\exp(jk\sqrt{\rho+\zeta})}{\rho+\zeta}\,\mathrm{d}\rho\,\mathrm{d}\theta\,, \qquad (2)$$

where $\rho = r^2$, $\zeta = z^2$, and $f'(\rho,\theta)$ is the aperture function in the new coordinates. Equation (2) contains a correlation integral, and therefore by using the convolution theorem we can define a function $c(\zeta)$ from Eq. (2) as follows:

$$c(\zeta) = \frac{2j\lambda u(\zeta)}{\sqrt{\zeta}} = \int_{-\infty}^{\infty} T(v)H'^{*}(v)\exp(j2\pi v\zeta)\,\mathrm{d}v\,, \qquad (3)$$

where $T(v)$ and $H'(v)$ are the Fourier transforms of the $t(\rho)$ and $h'(\rho)$, respectively, and

$$t(\rho) = \int_0^{2\pi} f'(\rho,\theta)\,\mathrm{d}\theta\,, \qquad h'(\rho) = \frac{\exp(-jk\sqrt{\rho})}{\rho}\,. \qquad (4)$$

Next we explain the EPOCS algorithm. The EPOCS algorithm may start with an arbitrary random aperture function $t_0(\rho)$. In iteration i of the algorithm the aperture function $t_i(\rho)$ is projected onto the constraint set in the aperture plane. The precise definition of this projection, $P_1[t_i(\rho)]$, depends on the choice of constraints, which usually affects the magnitude distribution of $t_i(\rho)$ but not the phase distribution. [See, for example, Eq. (7) below]. The projected aperture is correlated with $h(\rho)$ to yield $c_i(\zeta)$, according to Eq. (3). In fact, we perform operations, as in the following expression: $c_i(\zeta) = \mathcal{F}^{-1}\{\mathcal{F}\{P_1[t_i]\}(H'^{*})\}$, where $\mathcal{F}$ is the Fourier transform. The result is projected onto the constraint set in the correlation plane, where the projection is defined by

$$P_2[c_i(\zeta)] = \begin{cases} 2\lambda\left[\dfrac{I_0(\zeta)}{\zeta}\right]^{1/2}\exp[j\Psi_i(\zeta)] & \zeta\in\Delta\zeta\,, \\ c_i(\zeta) & \text{otherwise} \end{cases} \qquad (5)$$

where $\Psi_i(\zeta)$ is the phase distribution of $c_i(\zeta)$. According to Eq. (5), such a projection constrains the

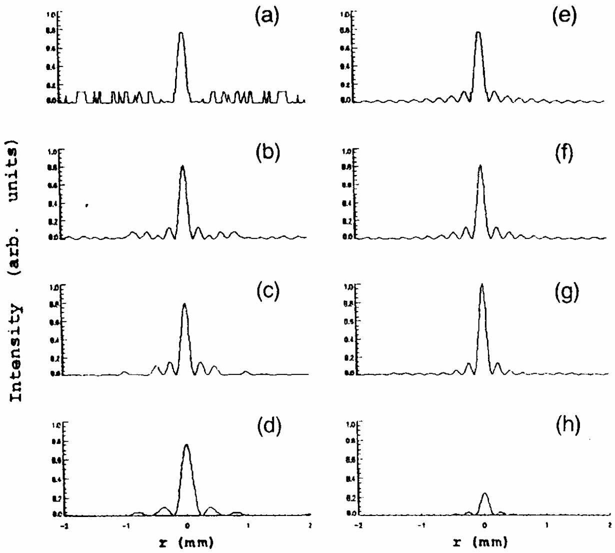

Fig. 1. Transverse intensity distribution of the beam obtained from (a)–(d) the EPOCS algorithm and (e)–(h) the Bessel beam $J_0(\alpha r)$ at $z = 0$ [(a), (e)], $z = 52$ cm [(b), (f)], $z = 104$ cm [(c), (g)], and $z = 156$ cm [(d), (h)].

intensity $|u(\zeta)|^2$ to be equal to $I_0(\zeta)$ along the interval $\Delta\zeta$. The next step is to return to the aperture plane, and we do this by calculating the $(i + 1)$ aperture function, using the formula $t_{i+1}(\rho) = \mathcal{F}^{-1}\{\mathcal{F}\{P_2[c_i]\}(H'^*)^{-1}\}$. These four operations repeat iteratively, while in every iteration we calculate the error function

$$e_i = \frac{1}{\Delta\zeta}\int_{\Delta\zeta} |c_i(\zeta) - P_2[c_i(\zeta)]|^2 \, d\zeta\,. \tag{6}$$

This expression is taken to reflect the performance of the aperture $t_i(\rho)$. We convert the final obtained aperture to a two-dimensional aperture function by the coordinates transform $t(\rho) \rightarrow t(r)$ and then by making a rings function $f(r,\theta)$, where the value of each ring of radius r is equal to $t(r)$.

As we proceed, are we assured of convergence of the error function? In the present state of the algorithm we cannot say much about its convergence properties, except to remark that it has worked well with many examples. The correlation here is not an energy-converging process; therefore we cannot prove the nondiverging property[14] of the EPOCS. However, in the Fresnel approximation there is a Fourier relation between an aperture and the axial distribution,[15] and therefore the energy is conserved in passing between the domains in this approximation. The principal point is that the synthesis of the axial profile can be declared a simple optimization problem. There are many algorithms that can solve this problem, and we have picked one that seemed to us to be easy, rapid, and successful in the sense that the optimal result (local optimum) yielded an error less than the error of the Bessel beam. This comparison is demonstrated next.

Let us try the proposed approach by considering a nondiffracting beam and comparing the results from EPOCS with those of the Bessel beam.[1] The desired output distribution is $I_0(z) =$ constant along some longitudinal interval Δz. In order to make a fair comparison we take the transverse distribution of the field in the plane $z = 0$ to have the central lobe of a Bessel function $J_0(\alpha r)$. The radius of the central lobe is $w_0 = 150$ μm ($\alpha = 160$ cm^{-1}), and it is surrounded by a low background level up to some limited radius $r_0 = 2$ mm. The maximum absolute value of the background level, s, is determined to be equal to the maximum absolute value of the first sidelobe of the Bessel function ($s \approx 0.4$). This can be summarized by the projection formula

$$P_1[t_i(\rho)] = \begin{cases} J_0(\alpha\sqrt{\rho}) & 0 < \sqrt{\rho} < w_0 \\ s\exp[j\phi_i(\rho)] & t_i(\rho) > s \wedge w_0 < \sqrt{\rho} < r_0\,, \\ t_i(\rho) & t_i(\rho) \le s \wedge w_0 < \sqrt{\rho} < r_0 \\ 0 & \sqrt{\rho} > r_0 \end{cases} \tag{7}$$

where $\phi_i(\rho)$ is the phase distribution of $t_i(\rho)$. The compared Bessel distribution $J_0(\alpha r)$ is shown in Fig. 1(e), and in this experiment the concerned interval Δz is 1.5 m. This choice is made here arbitrarily, but, as we know from many computer experiments, the larger we choose Δz, the greater the error is likely to be of the EPOCS algorithm at the ith iteration.

The transverse intensity of the EPOCS beam, shown in Fig. 1(a), was obtained after ~1000 iterations of the EPOCS algorithm. Transversal cross sections of the two beams for $\lambda = 0.5$ μm are depicted in Figs. 1(a)–1(d) for the synthetic beam and Figs. 1(e)–1(h) for the Bessel beam, at four different distances from the aperture. The axial intensity $|u(z)|^2$ of the beam diffracted from that aperture [Fig. 1(a)] is shown in Fig. 2(a). For comparison the performance of the Bessel beam is shown in Fig. 2(b). These results demonstrate that the new nondiffracting beam is closer to a constant level for a longer longitudinal interval compared with Durnin's beam.

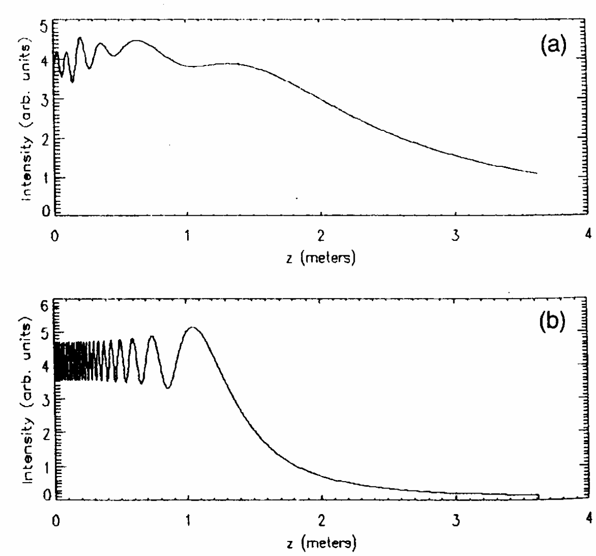

Fig. 2. Intensity distribution along the propagation axis of the beam obtained from (a) the EPOCS algorithm and (b) the Bessel aperture $J_0(\alpha r)$.

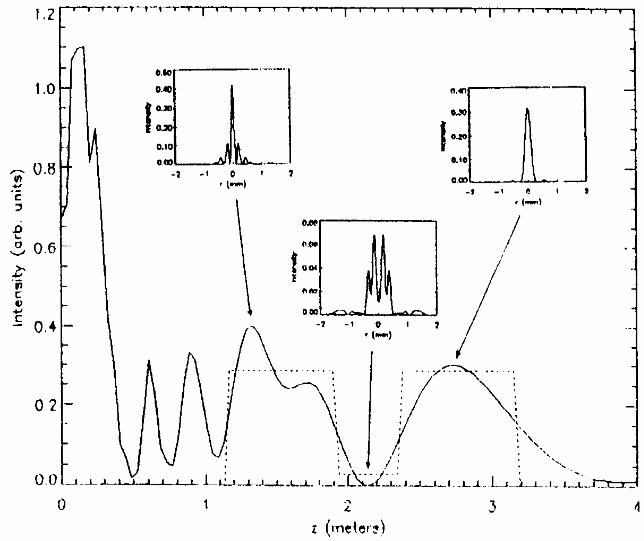

Fig. 3. Intensity distribution along the propagation axis of the beam diffracted from a phase-only aperture (solid curve) calculated by the EPOCS. The dotted curve is the requested profile $I_0(z)$, and the insets show the transverse cross sections of the intensity at three points along the z axis.

In other words, an aperture with the same dimensions of a Bessel beam (same central lobe, overall width, and background maximum value) yields a nondiffracting beam for a longer distance and with a greater accuracy compared with the performance of that Bessel beam.

For the second example we choose different constraints in both domains. In the aperture plane the desired distribution is a phase-only function, and therefore the projection is

$$P_1[t_i(\rho)] = \begin{cases} \exp[j\phi_i(\rho)] & \sqrt{\rho} < r_0 \\ 0 & \text{otherwise} \end{cases}, \qquad (8)$$

where $r_0 = 2$ mm, as in the first example. The axial distribution chosen this time is not constant but some other profile shown in Fig. 3 by the dotted curve (the controlled interval is between $z = 112$ cm and $z = 319$ cm). The axial intensity distribution diffracted from the phase-only aperture is shown in Fig. 3 by the solid curve. This aperture was obtained after 500 iterations of the EPOCS algorithm. The transverse cross sections at various points along the z axis are depicted also in Fig. 3.

In conclusion, we have demonstrated a way to direct the diffraction distribution along the optical axis emitted from any given aperture. In particular, we considered, as an example, the nondiffracting beam, where the transversal distribution in the plane $z = 0$ was a narrow intense central lobe supported by weak wide background illumination. The performance of this beam seemed to be better than that of the Bessel nondiffracting beam. Our beam distribution was not connected to any specific family of functions such as the Bessel functions. That means that the beam could be shaped in any form by many kinds of constraints. For instance, guided by practical considerations, we may require a binary distribution for the background illumination of the beam. Finally it should be mentioned that our method can be generalized to reshape any longitudinal intensity profile, or even any longitudinal complex amplitude profile, at least for a short interval. All these subjects are of great interest for future research, and we may expect to see them in the literature soon.

It is a great pleasure to thank Joseph L. Horner, Rome Laboratory, for his support and Raphael Trifon, Technion, Haifa, Israel, for his valuable comments. This study was done while the author was a National Research Council Research Associate at Rome Laboratory.

*Present address, Department of Applied Physics, Mail Stop 128-95, California Institute of Technology, Pasadena, California 91125.

References

1. J. Durnin, J. Opt. Soc. Am. A **4,** 651 (1987).
2. F. Gori, G. Guattari, and C. Padovani, Opt. Commun. **64,** 491 (1987).
3. F. Bloisi and L. Vicari, Opt. Commun. **75,** 353 (1990).
4. P. L. Overfelt and C. S. Kenney, J. Opt. Soc. Am. A **8,** 732 (1991).
5. A. J. Cox and J. D'Anna, Opt. Lett. **17,** 232 (1992).
6. J. Durnin, J. J. Miceli, Jr., and J. H. Eberly, Phys. Rev. Lett. **58,** 1499 (1987).
7. G. Indebetouw, J. Opt. Soc. Am. A **6,** 150 (1989).
8. A. Vasara, J. Turunen, and A. T. Friberg, J. Opt. Soc. Am. A **6,** 1748 (1989).
9. J. K. Jabczynski, Opt. Commun. **77,** 292 (1990).
10. R. M. Herman and T. A. Wiggins, J. Opt. Soc. Am. A **8,** 932 (1991).
11. A. J. Cox and D. C. Dibble, J. Opt. Soc. Am. A **9,** 282 (1992).
12. J. W. Goodman, *Introduction to Fourier Optics,* 1st ed. (McGraw-Hill, New York, 1968), Chap. 3, p. 42.
13. H. Stark, ed., *Image Recovery Theory and Application,* 1st ed. (Academic, New York, 1987), Chap. 8, p. 277.
14. J. Rosen, Opt. Lett. **18,** 1183 (1993).
15. B. Colombeau, C. Froehly, and M. Vampouille, Opt. Commun. **28,** 35 (1979).